Applied Catalysis B: Environmental 160–161 (2014) 344–355

Contents lists available at ScienceDirect

Applied Catalysis B: Environmental

journal homepage: www.elsevier.com/locate/apcatb

Highly active Ni_2P/SiO_2 catalysts phosphorized by triphenylphosphine in liquid phase for the hydrotreating reactions

Junen Wang, Hui Chen, Yuchuan Fu, Jianyi Shen*

Laboratory of Mesoscopic Chemistry, School of Chemistry and Chemical Engineering, Nanjing University, Nanjing 210093, China

ARTICLE INFO

Article history:
Received 3 March 2014
Received in revised form 18 April 2014
Accepted 20 May 2014
Available online 29 May 2014

Keywords:
Supported Ni_2P
Triphenylphosphine
Liquid phase phosphidation
Microcalorimetric adsorption of CO
Hydrotreating reactions

ABSTRACT

A highly loaded and dispersed 60%Ni/SiO_2 catalyst was phosphorized by triphenylphosphine (PPh_3) in liquid phase for the preparation of highly loaded and dispersed Ni_2P/SiO_2 catalysts. It was found that without pre-reduction, the Ni/SiO_2 was difficult to be phosphorized by PPh_3, and large Ni_2P particles were resulted at the high phosphidation temperatures (543–593 K). When the Ni/SiO_2 was pre-reduced, the highly dispersed nano nickel particles formed were easily phosphorized by PPh_3 at the lower temperatures (443–543 K). The resulted Ni_2P/SiO_2 catalyst phosphorized by PPh_3 at 443 K possessed small and homogeneous Ni_2P particles (~6 nm) with the high Ni_2P active site density (324 μmol/g) as titrated by the adsorption of CO. It was significantly more active than the Ni_2P/SiO_2 catalyst phosphorized by PH_3 in gas phase with the Ni_2P active site density of 263 μmol/g for the hydrodesulphurization of dibenzothiophene and hydrogenation of tetralin to decalin in a model diesel.

1. Introduction

The hydrotreating of transportation fuels has become increasingly important as a result of the severer environmental protection laws in many countries that requires <10 ppm sulfur in gasoline and diesel [1]. The traditional hydrotreating catalysts are not adequate to meet the regulated levels, and this has given rise to great efforts to search for appropriate hydrodesulfurization (HDS) catalysts. Transition metal phosphides were found to exhibit the high activities for the reactions of hydrodesulfurization and hydrodenitrogenation (HDN). Oyama et al. [2] found that the activity of metal phosphides for the HDS of dibenzothiophene (DBT) followed the order of $Ni_2P > WP > MoP > CoP > Fe_2P$ and that Ni_2P/SiO_2 catalysts were significantly more active than the traditional HDS catalysts $CoMoS/Al_2O_3$ and $NiMoS/Al_2O_3$.

There were quite a few methods for the preparation of transition metal phosphides, in which temperature-programmed-reduction (TPR) was the one often used [3–7]. In this method, the precursors containing transition metals and phosphates were reduced by H_2. The method is simple, but needs high temperatures so that the metal phosphides formed usually exhibit large particles with low HDS activities [8]. In addition, excessive phosphorous oxides (PO_x) may exist on the catalyst surfaces, affecting the HDS activity [9]. The thermal decomposition of hypophosphites in an inert atmosphere is another method for the preparation of transition metal phosphides [10–12]. In this method, the temperatures required are not high so that small particles of metal phosphides can be produced. However, large quantities of impurities such as phosphates may be remained in the catalysts and must be removed by washing with water, causing the burdens of post-treatments.

In recent years, a liquid synthesis method was developed for the preparation of metal phosphides. In this method, soluble transition metal salts, metal complexes and organic phosphorous (or elementary P) were mixed and reacted under an inert atmosphere. The phosphorous source usually used in this method included white phosphorous (P_4) [13–15], tris(trimethylsilyl)phosphine ($P(SiMe_3)_3$) [16–18], trioctyl phosphine (TOP) [19–22], trioctyl phosphine oxide (TOPO) [23] and triphenylphosphine (PPh_3) [24,25]. The temperatures used in this liquid synthesis method were usually low and metal phosphides with different morphologies could be prepared [26]. However, coordination agents were usually needed in this method, which were unfavorable for catalytic reactions and must be removed by the post-treatments. Senevirathne et al. [27] synthesized Ni_2P by the liquid method and investigated the effect of $CHCl_3$ on the HDS activity. They found that the activity of Ni_2P was greatly increased after the removal of $CHCl_3$ by washing. As compared to the TPR method, the liquid synthesis method may be used at low temperatures to synthesize small particles of metal phosphides with controlled morphologies. Nevertheless, the liquid synthesis method had the complex process and used expensive organic compounds so that it might not be suitable for the large scale synthesis of metal phosphides. In

* Corresponding author. Tel.: +86 25 83594305; fax: +86 25 83594305.
E-mail address: jyshen@nju.edu.cn (J. Shen).

http://dx.doi.org/10.1016/j.apcatb.2014.05.038
0926-3373/

addition, the method did not seem to be suitable for the preparation of supported metal phosphides [28,29].

It is well known that there are two sulfidation methods for the industrial HDS catalysts such as CoMoS and NiWS, i.e., sulfidation in gaseous and liquid phases [30–34]. Inspired by this fact, we thought that metal phosphides could also be prepared by the phosphidation in gaseous and liquid phases. Previously, we phosphorized a 60%Ni/SiO_2 catalyst by PH_3 in gaseous phase and prepared a highly active Ni_2P/SiO_2 catalyst for the hydrotreating reactions [35]. In this work, Ni_2P/SiO_2 catalysts were prepared by the phosphidation of the 60%Ni/SiO_2 by PPh_3 in liquid phase at the relatively low temperatures. In this way, the advantages of liquid phase phosphidation were remained while the disadvantages of the method (e.g., use of coordination agents) were avoided. After the optimization of phosphidation conditions, highly active Ni_2P/SiO_2 catalysts were prepared and exhibited the high activities for the HDS of DBT, HDN of quinoline and hydrogenation of tetralin.

2. Experimental

2.1. Preparation of catalysts

A Ni/SiO_2 catalyst with about 60 wt% Ni was prepared by the co-precipitation method and dried with *n*-butanol [35,36]. In short, $Ni(NO_3)_2{\cdot}6H_2O$ was dissolved in 100 ml de-ionized water to obtain a solution. $Na_2SiO_3{\cdot}9H_2O$ and Na_2CO_3 were dissolved in 100 ml de-ionized water to obtain another solution. The two solutions were added drop-wise into 200 ml de-ionized water under stirring at 353 K. A green precipitate was formed, filtered and washed thoroughly. 200 ml *n*-butanol was then added into the precipitate and evaporated at 353 K. The precipitate was then further dried at 393 K for 12 h.

Above catalyst could be directly phosphorized without the pre-reduction. Specifically, the 60%Ni/SiO_2 was first calcined in air at 673 K for 3 h. It was then loaded into a micro-reactor with the inner diameter of 10 mm and sandwiched with quartz sands. H_2 (0.1 MPa and 40 ml/min) was flown through the catalyst bed and the reactor temperature was raised with a ramp rate of 1 K/min to 373 K, at which a heptane solution containing 4% PPh_3 was pumped into the reactor with a liquid hourly space velocity (LHSV) of 2 h^{-1} and H_2/oil of 300 v/v. The reactor was further heated to different temperatures (443–643 K) at which the catalyst was phosphorized by PPh_3 for 16 h. Then, feeding heptane solution of PPh_3 was stopped and the temperature was further increased to 673 K, at which the catalyst was heated in H_2 for 3 h. The catalyst was then cooled down to a reaction temperature, at which the model diesel was pumped into the reactor and the hydrotreating reactions began. The catalysts phosphorized directly in liquid phase without the pre-reduction were denoted as NiP/SiO_2-DLP*xxx*, in which *xxx* was the phosphidation temperature. For example, NiP/SiO_2-DLP593 represented the Ni_2P/SiO_2 catalyst phosphorized by PPh_3 directly in liquid phase at 593 K without the pre-reduction.

Above catalyst could also be phosphorized after the pre-reduction. Specifically, the 60%Ni/SiO_2 was also first calcined in air at 673 K for 3 h. It was then loaded into the micro-reactor and reduced in H_2 (0.1 MPa and 40 ml/min) at 673 K for 2 h. Then, the catalyst was cooled down to phosphidation temperatures (393–643 K) at which the catalyst was phosphorized with PPh_3 (4%) in heptane solution (LHSV of 2 h^{-1} and H_2/oil of 300 v/v) for 16 h. The further treatment was the same as the process of direct phosphidation (treated in H_2 at 673 K for 3 h) before the catalyst was cooled down to the reaction temperatures for the hydrotreating reactions. The catalysts phosphorized by PPh_3 in liquid phase after the pre-reduction were denoted as NiP/SiO_2-RLP*xxx*, in which *xxx* was the phosphidation temperature. For example, NiP/SiO_2-RLP443 represented the Ni_2P/SiO_2 catalyst phosphorized by PPh_3 in liquid phase at 443 K after the pre-reduction.

2.2. Characterization of catalysts

The Ni_2P/SiO_2 catalysts phosphorized by using PPh_3 in liquid phase were prepared separately for characterizations. The phosphidation processes were the same as those described above (Section 2.1). After the phosphidation, the catalysts were further treated in H_2 at 673 K for 3 h. Then, the catalysts were passivated at room temperature for 12 h under N_2 containing about 0.5 vol% O_2, before they were characterized with different techniques.

N_2 adsorption–desorption measurements were carried out at 77.3 K using a Micromeritics Gemini V 2380 autosorption analyzer. The specific surface areas were calculated according to the Brunauer–Emmett–Teller (BET) equation while pore distributions were obtained by the Barret–Joyner–Halenda (BJH) method. Samples were degassed in flowing N_2 at 473 K for 5 h before the measurements.

X-ray diffraction (XRD) patterns were collected on a Shimadzu XRD-6000 powder diffractometer (Japan) using a Cu $K\alpha$ radiation (λ = 0.1541 nm). The 2θ scans covered the range of 10 to 80° with a step of 0.02°.

The chemical compositions of catalysts were analyzed by an ARL-9800 X-ray fluorescence spectrometer (XRF).

The microcalorimetric adsorption of CO was performed by using a Setaram Tian-Calvet C-80 heat-flux microcalorimeter, connected to a gas-handling system equipped with a Baratron capacitance manometer for precise pressure measurements. Samples were reduced in flowing H_2 at 673 K for 3 h and evacuated at 673 K for 1 h before the measurements. Microcalorimetric adsorption was performed at 308 K.

Transmission electron microscope (TEM) was performed using a JEOL JEM-2100 high-resolution microscope operating at 200 kV. The samples were dispersed in 5% ethanol solution and dropped onto a copper grid coated with a carbon film.

2.3. Catalytic tests

Catalytic tests were carried out for the HDS of DBT, HDN of quinoline and hydrogenation of tetralin in a model diesel containing 1.72% DBT (3000 ppm S), 0.185% quinoline (200 ppm N), 5% tetralin and 0.5% *n*-octane (as an internal standard) in balanced *n*-tetradecane (solvent). A fix-bed reactor was used to perform the reactions. The reactions were carried out at 3.1 MPa with LHSV of 2 h^{-1} and H_2/oil ratio of 1500 (v/v). The catalytic activity was measured at different reaction temperatures. The reactant solution was fed into the reactor through a high pressure syringe pump. The products were collected after 24 h when the activity was stabilized and analyzed on two gas chromatographs. One was equipped with two SE-30 capillary columns connected to a flame ionization detector (FID) and a flame photometric detector (FPD) for the analysis of hydrocarbons and DBT, respectively. Another gas chromatograph was equipped with a SE-54 capillary column and a nitrogen–phosphorus detector (NPD) for the analysis of quinoline.

3. Results and discussion

3.1. Direct phosphidation (without pre-reduction)

The 60%Ni/SiO_2 catalyst can be either phosphorized directly without the reduction or phosphorized after the reduction. Thus, the effect of reduction on the resulted Ni_2P/SiO_2 catalysts was investigated in this work.

Fig. 1 shows the XRD patterns of the Ni_2P/SiO_2 catalysts phosphorized directly by PPh_3 after the calcination at 673 K (without the

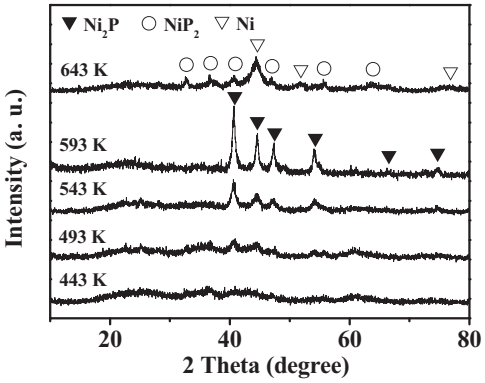

Fig. 1. XRD patterns for the Ni_2P/SiO_2 catalysts obtained by the direct phosphidation of the 60%Ni/SiO_2 (without the pre-reduction) using PPh_3 in the liquid phase at different temperatures indicated.

pre-reduction). The phosphidation was performed in liquid phase at the temperatures from 443 to 643 K. All the samples exhibited a broad and weak peak around 22°, belonging to amorphous SiO_2. No diffraction peaks of Ni_2P were observed for the sample NiP/SiO_2-DLP443, indicating that the temperature (443 K) might be too low so that the degree of phosphidation was low and the Ni_2P particles formed were too small to be detected by XRD. Three weak diffraction peaks around 40.7°, 44.6° and 47.4°, characteristic of Ni_2P (PDF 65-1989), appeared for the sample NiP/SiO_2-DLP493. The intensities of these diffraction peaks for Ni_2P increased with the increase of phosphidation temperatures from 493 to 593 K. When the Ni/SiO_2 catalyst was phosphorized at 643 K, diffraction peaks of NiP_2 (PDF 21-0590) and Ni (PDF 65-2855) appeared, besides those of Ni_2P. Senevirathne et al. [27,37] observed the similar phenomenon. These results indicated that the 60%Ni/SiO_2 catalyst could be directly phosphorized by PPh_3 in liquid phase without the pre-reduction for the formation of Ni_2P/SiO_2 catalysts. The formation of metal phosphides by the phosphidation of metal oxides using PH_3 and TOP has been reported previously [8,38]. However, the direct phosphidation of metal oxides using PPh_3 has not been reported before.

Fig. 2 shows the TEM images of the catalyst 60%Ni/SiO_2 after calcination at 673 K (a), as well as the NiP/SiO_2-DLP493 (b) and NiP/SiO_2-DLP593 (c) obtained by the phosphidation of 60%Ni/SiO_2 with PPh_3 in liquid phase at 493 and 593 K, respectively. No particles (Fig. 2(a)) were observed for the 60%Ni/SiO_2 after calcination at 673 K, indicating the high dispersion of nickel species. In fact, no crystalline phases could be detected by XRD (not shown), indicating the well dispersed Ni^{2+} and Si^{4+}. After the phosphidation at 493 K, Ni_2P particles could be clearly seen (Fig. 2(b)) with the wide distribution of particle sizes (5–30 nm). However, the XRD peaks of this sample were weak and broad, indicating the existence of quite a few small Ni_2P particles. The average particle size was estimated to be about 8.3 nm according to the Scherrer equation, consistent with the TEM result. After the phosphidation at 593 K, the Ni_2P particles formed became bigger (Fig. 2(c)) with sizes from 5 to 40 nm. The average particle size was estimated to be about 14.1 nm according to the Scherrer equation, again consistent with the TEM result. The average particle size of Ni_2P was estimated to be about 9.2 nm for the NiP/SiO_2-DLP543 according to the Scherrer equation (see Table 1).

The adsorption of CO can be used to probe the densities of active sites on the surface of Ni_2P catalysts [35,39]. The heats for the adsorption of CO on the surface of Ni_2P can be measured at the same time [35,40]. Fig. 3 shows the isotherms and differential heats for the adsorption of CO on the NiP/SiO_2-DLP493, NiP/SiO_2-DLP543 and NiP/SiO_2-DLP593. The initial heats were found to be similar

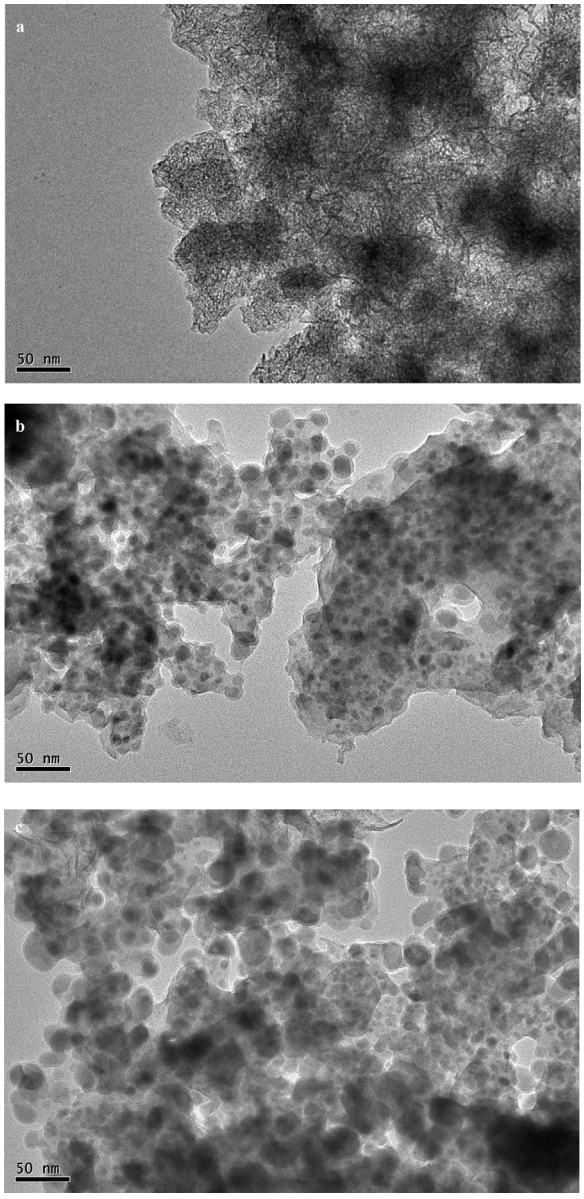

Fig. 2. TEM images of the 60%Ni/SiO_2 catalyst after calcination at 673 K (a), followed by the direct phosphidation using PPh_3 in the liquid phase at 493 K (b) and 593 K (c), respectively.

(~84 kJ/mol) for the adsorption of CO on these samples, indicating the similar surface composition and chemical properties. However, the uptakes of CO on these samples were significantly different (62, 104 and 124 μmol/g on the NiP/SiO_2-DLP493, NiP/SiO_2-DLP543 and NiP/SiO_2-DLP593, respectively). The uptake of CO increased with the increase of phosphidation temperature in the range of 493–593 K, indicating the increase of Ni_2P content in the samples. The NiP/SiO_2-DLP593 possessed the most surface active sites, and thus it should be the most active among this series of catalysts.

Table 1 summarizes the information about the surface areas, pore parameters, crystalline phases, average particle sizes and CO uptakes for the series of NiP/SiO_2-DLP catalysts. The surface area and pore volume were decreased while the pore size was increased with the increase of phosphidation temperature. At the same, the particle size of Ni_2P increased from 8.3 to 14.1 nm while the CO uptake increased from 62 to 124 μmol/g, with the increase of phosphidation temperature from 493 to 593 K. Apparently, more nickel would be phosphorized and larger Ni_2P particles would be formed

Table 1
Textural and structural properties of Ni_2P/SiO_2 catalysts phosphorized directly using PPh_3 in the liquid phase at different temperatures.

Phosphoriz. temp.	443 K	493 K	543 K	593 K	643 K
S_{BET} (m^2/g)	172	136	98	93	68
Pore volume (cm^3/g)	0.5	0.64	0.52	0.43	0.38
Pore size (nm)	7.6	12.4	14.8	15.1	17.6
XRD phase	No clear phase detected	Ni_2P	Ni_2P	Ni_2P	Ni_2P, NiP_2, Ni
D (nm)	–	8.3	9.2	14.1	8.7, 7.3, 6.3
CO uptake (μmol/g)	–	62	104	124	–

Note: *D* was estimated by the Scherrer equation according to the full width at half maximum (FWHM) of the peak at 40.7° in the XRD patterns shown in Fig. 1.

with the increase of phosphidation temperature. Some nickel could not be phosphorized and detected by XRD so that their amounts and valent states (reduced or oxidized) were not known. In fact, nickel in the 60%Ni/SiO_2 could not be completely reduced even in H_2 at 673 K, and the reducibility of nickel was determined by the H_2—O_2 titration [36]. Thus, it is highly possible that quite a few nickel species might not be reduced and phosphorized in the NiP/SiO_2-DLP catalysts.

Metallic nickel, Ni_2P and NiP_2 were detected in the sample NiP/SiO_2-DLP643. The existence of Ni in this sample might be due to that the disproportionation of Ni_2P to Ni and NiP_2 occurred at the high temperature (643 K) or only the small particles of metallic nickel could be phosphorized. The disproportionation of Ni_2P seemed unlikely since no metallic nickel was detected in the NiP/SiO_2-RLP-643 phosphorized at 643 K by PPh_3 in liquid phase after the pre-reduction (the results will be presented shortly below). On the other hand, when the direct phosphidation was performed on the calcined Ni/SiO_2 catalyst, the nickel species must be first reduced and then phosphorized. At the low temperatures, only small amount of nickel could be reduced and phosphorized, and thus the catalysts possessed the low densities of surface active sites.

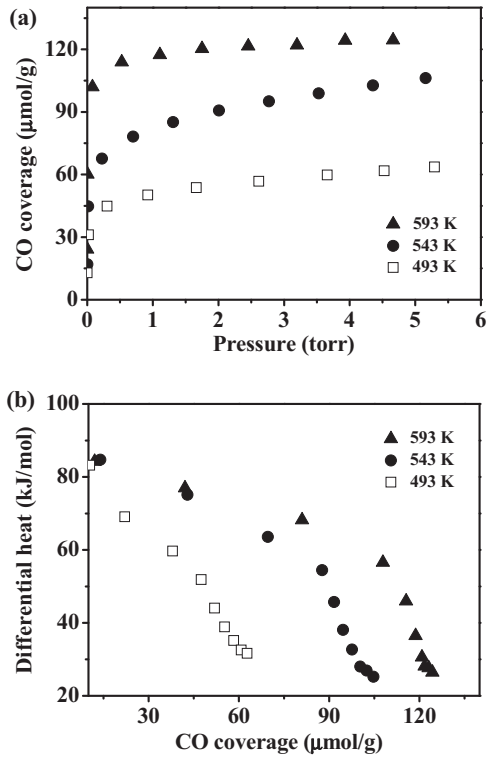

Fig. 3. Isotherms (a) and differential heats (b) measured for the adsorption of CO at 308 K on the Ni_2P/SiO_2 catalysts obtained by the direct phosphidation of the 60%Ni/SiO_2 catalyst using PPh_3 in the liquid phase at different temperatures indicated. Before the adsorptions, the samples were reduced at 673 K in H_2 for 2 h, followed by the evacuation at 673 K for 1 h.

At the high temperatures (e.g., 643 K), more nickel species could be reduced, but the nickel particles might be also grown larger so that the cores of these large particles could not be phosphorized. The formation of NiP_2 might be caused by the over-phosphidation at the high temperature (643 K). In fact, both the NiP/SiO_2-DLP-643 and NiP/SiO_2-RLP-643 phosphorized at 643 K contained NiP_2.

The activities of the NiP/SiO_2-DLP catalysts phosphorized directly for the HDS of DBT were displayed in Fig. 4. It is seen that the activities were increased with the increase of phosphidation temperature from 493 to 593 K, in consistence with their CO uptakes, i.e., the activity was higher over the NiP/SiO_2-DLP catalyst with the higher density of active sites of Ni_2P. The NiP/SiO_2-DLP593 exhibited the highest density of active sites and thus the highest activity for the HDS of DBT among this series of catalysts. The conversion of DBT reached 30 and 95% over the NiP/SiO_2-DLP593 at 513 and 613 K, respectively. However, the NiP/SiO_2-DLP643 phosphorized at 643 K possessed the significantly lower activity for the HDS of DBT, probably owing to the larger particles of Ni_2P formed and the other nickel phases (metallic Ni and NiP_2) in the catalyst caused by the phosphidation at the high temperature (643 K).

As compared with the Ni_2P/SiO_2 catalysts prepared by the TPR method, the Ni_2P/SiO_2 catalysts phosphorized directly by PPh_3 in liquid phase (NiP/SiO_2-DLP) were significantly more active for the HDS of DBT. For example, at 573 K, the conversion of DBT was 76% over the NiP/SiO_2-DLP593 while it was only 40% over the Ni_2P/SiO_2 catalyst prepared by the TPR method [35].

The activities of the NiP/SiO_2-DLP catalysts phosphorized directly for the HDN of quinoline were presented in Fig. 5. Again, the activities were increased with the increase of phosphidation temperature from 493 to 593 K, in consistence with their HDS activities, indicating that the catalyst with more active sites of Ni_2P (as titrated by CO adsorption) was more active for the HDN reaction. The NiP/SiO_2-DLP593 exhibited the highest activity for the HDN of quinoline among this series of catalysts. The conversion of quinoline reached 100% over the NiP/SiO_2-DLP593 at 573 K. The

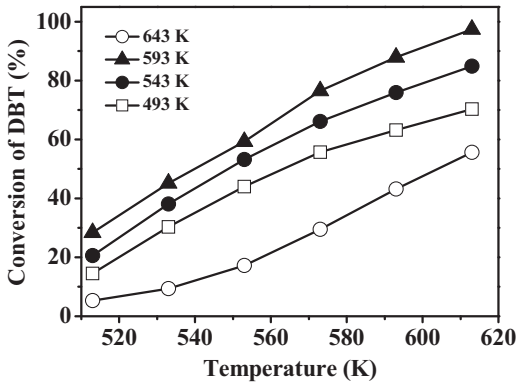

Fig. 4. Conversions of DBT (HDS) on the Ni_2P/SiO_2 catalysts obtained by the direct phosphidation of the 60%Ni/SiO_2 using PPh_3 in the liquid phase at different temperatures indicated. Reaction conditions: *P* = 3.1 MPa, LHSV = 2 h^{-1} and H_2/oil = 1500 (v/v).

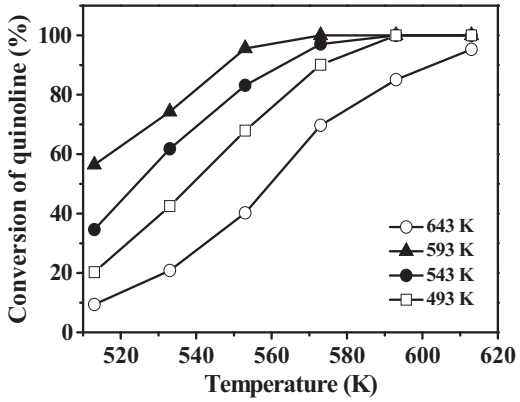

Fig. 5. Conversions of quinoline (HDN) on the Ni_2P/SiO_2 catalysts obtained by the direct phosphidation of the 60%Ni/SiO_2 using PPh_3 in the liquid phase at different temperatures indicated. Reaction conditions: P = 3.1 MPa, LHSV = 2 h^{-1} and H_2/oil = 1500 (v/v).

NiP/SiO_2-DLP643 had the much lower activity for the HDN of quinoline, in consistence with its HDS activity. The reason was the same as described above.

Similarly, the Ni_2P/SiO_2 catalysts phosphorized directly by PPh_3 in liquid phase (NiP/SiO_2-DLP) were significantly more active for the HDN of quinoline than the Ni_2P/SiO_2 catalysts prepared by the TPR method. At 573 K, the conversion of quinoline was 100% over the NiP/SiO_2-DLP593 while it was only 72% over the Ni_2P/SiO_2 catalyst prepared by the TPR method [35].

The content of aromatic hydrocarbons in diesel fuels is an important factor determining the quality of fuels. Hydrocarbons with multi-rings have low cetane numbers and produce more particulate matters (PM) from diesel engines [41]. In this work, the hydrogenation of tetralin was employed to probe the activity of Ni_2P/SiO_2 catalysts for the hydrogenation of aromatic rings. Fig. 6 shows the results. At the relatively low temperatures, the conversions of tetralin were low for the NiP/SiO_2-DLP catalysts. At 613 K, the difference in the activity of hydrogenation of tetralin was apparent over the different NiP/SiO_2-DLP catalysts. The conversion of tetralin was measured to be 9, 13, 18 and 8% at 613 K over the NiP/SiO_2-DLP493, NiP/SiO_2-DLP543, NiP/SiO_2-DLP593 and NiP/SiO_2-DLP643, respectively, in consistence with their HDS and HDN activities. The NiP/SiO_2-DLP593 exhibited the much higher activity for the hydrogenation of tetralin than the Ni_2P/SiO_2 prepared by the TPR method (18 and 3% conversions of tetralin at 613 K [35]).

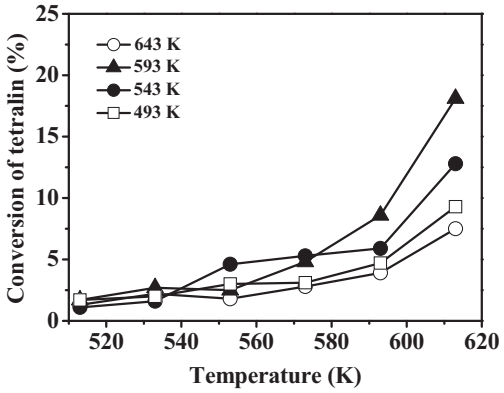

Fig. 6. Conversions of tetralin (hydrogenation) on the Ni_2P/SiO_2 catalysts obtained by the direct phosphidation of the 60%Ni/SiO_2 using PPh_3 in the liquid phase at different temperatures indicated. Reaction conditions: P = 3.1 MPa, LHSV = 2 h^{-1} and H_2/oil = 1500 (v/v).

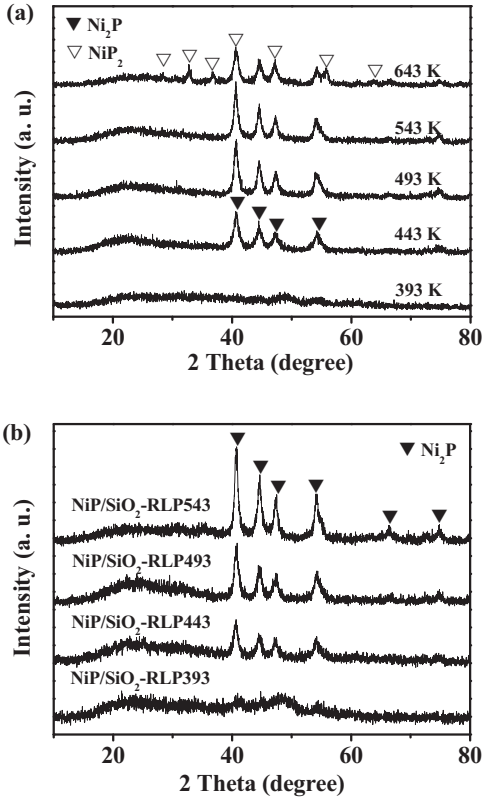

Fig. 7. XRD patterns of the fresh (a) and used (b) NiP/SiO_2-RLP catalysts. Reaction conditions: T = 513–613 K, P = 3.1 MPa, LHSV = 2 h^{-1} and H_2/oil = 1500 (v/v).

3.2. Phosphidation after reduction

The contents of Ni_2P formed by the direct phosphidation using PPh_3 might not be high enough owing to the low reducibility of nickel in this process, and the Ni_2P/SiO_2 catalysts prepared this way might not be highly active for the hydrotreating reactions. In this section, we present the results of phosphidation of the 60%Ni/SiO_2 catalyst by PPh_3 in liquid phase after it was reduced in H_2 at 673 K for 2 h.

Fig. 7(a) shows the XRD patterns of the Ni_2P/SiO_2 catalysts phosphorized by PPh_3 after the 60%Ni/SiO_2 catalyst was reduced. The phosphidation was performed in liquid phase at the temperatures from 393 to 643 K. No diffraction peaks of Ni_2P were observed for the sample NiP/SiO_2-RLP393, but some nickel must have been phosphorized since metallic nickel was observed before it was phosphorized [36]. In addition, XRF analysis indicated the presence of P in this sample (see Table 2). Four diffraction peaks around 40.7°, 44.6°, 47.4° and 54.2° attributed to Ni_2P (PDF 65-1989) were clearly seen for the sample NiP/SiO_2-RLP443. In contrast, the diffraction peaks of Ni_2P were hardly seen for the sample NiP/SiO_2-DLP443 (without the pre-reduction), indicating that the pre-reduction greatly promoted the formation of Ni_2P during the phosphidation process. With the increase of phosphidation temperature from 443 to 543 K, the intensities of these diffraction peaks of Ni_2P increased. When the Ni/SiO_2 catalyst was phosphorized at 643 K, significant amount of NiP_2 (PDF 21-0590) was formed, besides Ni_2P. This was similar to the situation of direct phosphidation at 643 K (see Fig. 1). However, the sample NiP/SiO_2-RLP643 did not contain metallic Ni, indicating that the presence of metallic Ni in the sample NiP/SiO_2-DLP643 was due to the incomplete phosphidation of large particles of Ni, not due to the disproportionation of Ni_2P. Thus, after the pre-reduction, the small particles of metallic Ni formed could be easily phosphorized even at the relatively low

Table 2
Textural and structural properties of Ni_2P/SiO_2 catalysts phosphorized using PPh_3 in the liquid phase at different temperatures after the 60%Ni/SiO_2 was pre-reduced in H_2 at 673 K for 2 h.

Phosphoriz. temp.	393 K	443 K	493 K	543 K	643 K
S_{BET} (m^2/g)	265	220	209	175	105
Pore volume (cm^3/g)	0.63	0.6	0.45	0.4	0.29
Pore size (nm)	6.3	7.7	8.6	6.3	9
XRD phase	–	Ni_2P	Ni_2P	Ni_2P	Ni_2P, NiP_2
D (nm)	–	6.2	7.8	8.4	8.2, 12.3
CO uptake (μmol/g)	465	324	302	250	101
Ni (wt%)	52.3	48.5	49.1	49.1	48.8
P (wt%)	8.3	13.2	14.1	16.4	17.8
P/Ni (atomic ratio)	0.3	0.52	0.54	0.63	0.69

Notes: *D* was estimated by the Scherrer equation according to the full width at half maximum (FWHM) of the peak at 40.7° in the XRD patterns shown in Fig. 7(a). The contents of Ni and P were analyzed by XRF.

temperature (443 K) for the formation of small Ni_2P particles with the homogeneous size (see below).

Fig. 7(b) presents the XRD patterns of some NiP/SiO_2-RLP catalysts after the hydrotreating reactions. Only the Ni_2P phase was observed in the used NiP/SiO_2-RLP-443, NiP/SiO_2-RLP-493 and NiP/SiO_2-RLP-543 catalysts, indicating the high stability of Ni_2P in the catalysts under the hydrotreating conditions at 513–613 K. No nickel sulfides were detected in these used catalysts, although there was study indicating the incorporation of S into the crystalline surface of Ni_2P during the hydrotreating reactions [42]. In addition, Ni_2P particles seemed larger (but not significantly) in the used catalysts as compared to the fresh ones, as evidenced by the increased intensities of the XRD peaks of Ni_2P (see Fig. 7(a)). There was the sign of presence of Ni_2P in the used NiP/SiO_2-RLP393 (with very weak Ni_2P peaks), indicating that the sample was indeed partially phosphorized although Fig. 7(a) shows that no Ni_2P was present in the fresh sample.

In order to know better the phases in the NiP/SiO_2-RLP393 and NiP/SiO_2-RLP443 after the hydrotreating reactions, we heat-treated the used samples at the high temperatures (773 and 823 K), with the hope that the particles in the two samples could be grown up to the extents that could be detected by XRD. The results are shown in Fig. 8.

Fig. 8(a) presents the XRD patterns for the used NiP/SiO_2-RLP393 after the treatments in N_2 and H_2 at 773 and 823 K, respectively. Since it was exposed in air after it was unloaded from the reactor, some nickel species in the sample might have been oxidized. Thus, strong diffraction peaks of NiO appeared for the sample after the treatments in N_2. In addition, weak diffraction peaks of Ni_9S_8 were observed in the sample after the treatments in N_2, indicating that the sample was not fully phosphorized and the un-phosphorized Ni metal might be converted into Ni_9S_8 (with low activity) during the hydrotreating reactions. Fig. 8(a) also shows that NiO was reduced to metallic Ni and Ni_9S_8 disappeared after the used sample was treated in H_2. Thus, Ni_9S_8 did not seem to be very stable since it could be reduced to Ni in H_2 at the high temperatures. At the same time, weak diffractions peaks of $Ni_{12}P_5$ appeared in the sample after the treatments in H_2, indicating that the sample was indeed partially phosphorized before the hydrotreating reactions.

Fig. 8(b) shows the XRD patterns for the used NiP/SiO_2-RLP443 after the treatments in N_2 and H_2 at 773 and 823 K, respectively. Although it was exposed in air after it was unloaded from the reactor, no phases of NiO and Ni_9S_8 were observed in the sample after the treatments in N_2. The main phase detected was Ni_2P with small amount of $Ni_{12}P_5$. This indicates that Ni_2P was highly stable since it remained after the hydrotreating reactions and then exposure to air. However, it was possible that O_2 might have adsorbed (for the formation of O_{ads}) on the surface of Ni_2P during its exposure in air. It was also possible that the adsorbed O_{ads} might react with Ni_2P to produce PO_4^{3-} and $Ni_{12}P_5$. When the sample was treated in H_2, the only phase detected was Ni_2P, even at the temperature as high as 823 K, indicating again the high stability of Ni_2P. During the H_2 treatments, the surface O_{ads} might be removed and the surface phosphates might be reduced to P that then reacted with $Ni_{12}P_5$ to produce Ni_2P.

The possible changes of phases in the used NiP/SiO_2-RLP393 and NiP/SiO_2-RLP443 when they were treated in N_2 and H_2 at the high temperatures may be expressed by the following processes:

$$Ni + O_{ads} \rightarrow NiO$$

$$Ni_9S_8 + 25\,O_{ads} \rightarrow 9\,NiO + 8\,SO_2$$

$$6\,Ni_2P + 4\,O_{ads} \rightarrow Ni_{12}P_5 + PO_4^{3-}$$

$$NiO + H_2 \rightarrow Ni + H_2O$$

$$Ni_9S_8 + 8\,H_2 \rightarrow 9\,Ni + 8\,H_2S$$

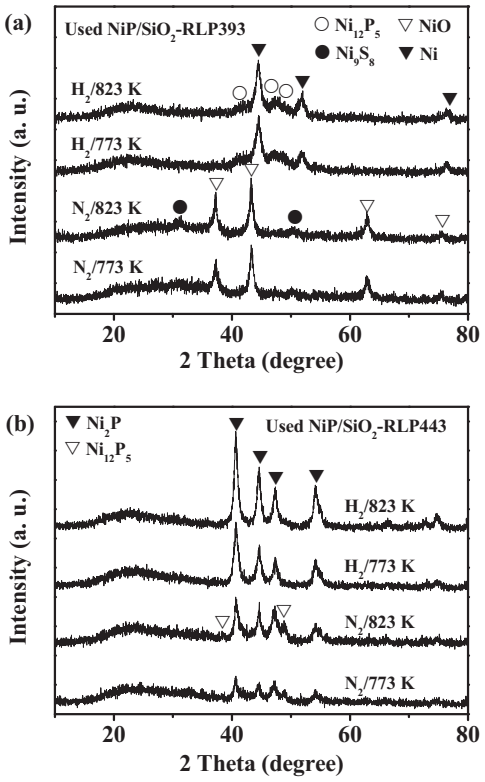

Fig. 8. XRD patterns for the used catalysts NiP/SiO_2-RLP393 (a) and NiP/SiO_2-RLP443 (b) after the treatments in N_2 and H_2 at 773 and 823 K, respectively, as indicated.

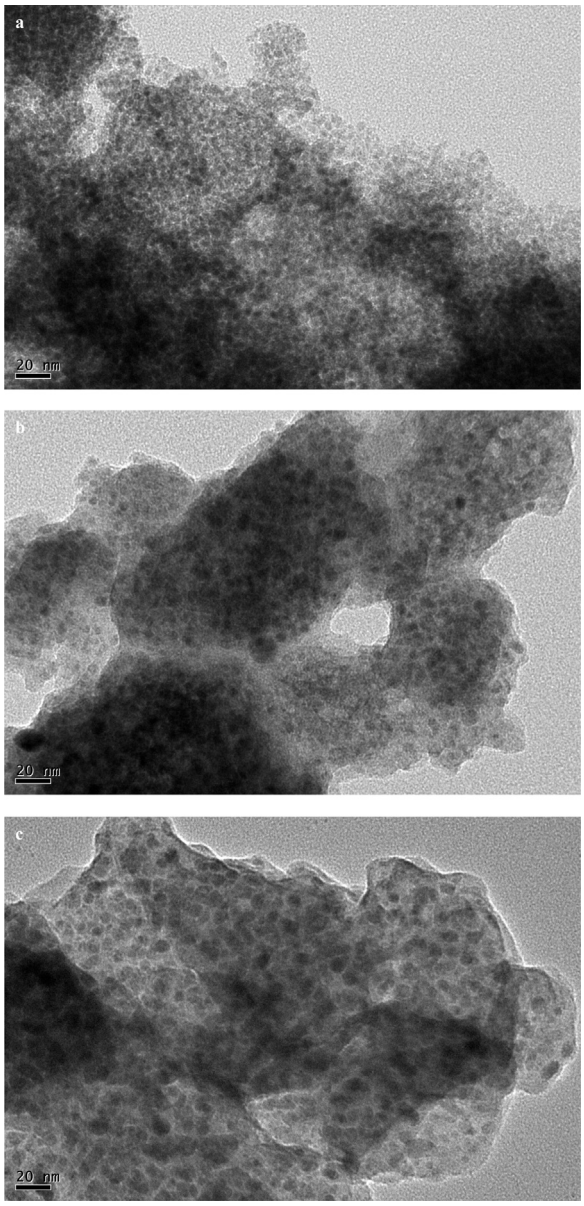

Fig. 9. TEM images of the 60%Ni/SiO_2 catalyst after the reduction in H_2 at 673 K for 2 h (a), followed by the phosphidation using PPh_3 in the liquid phase at 443 K (b) and 493 K (c), respectively.

$$Ni_{12}P_5 + PO_4{}^{3-} + 4\,H_2 \rightarrow 6\,Ni_2P + 4\,H_2O$$

Fig. 9 shows the TEM images of the 60%Ni/SiO_2 after reduction in H_2 at 673 K (a), as well as the NiP/SiO_2-RLP443 (b) and NiP/SiO_2-RLP493 (c) obtained by the phosphidation of reduced 60%Ni/SiO_2 with PPh_3 in liquid phase at 443 and 493 K, respectively. Many highly and homogeneously dispersed nano particles of metallic nickel were clearly seen in Fig. 9(a) for the 60%Ni/SiO_2 after the reduction. The average size of these nickel particles was about 3.6 nm. After the phosphidation by PPh_3 at 443 and 493 K, these Ni particles were turned into nano Ni_2P particles that were also highly and homogeneously dispersed as seen in Fig. 9(b and c). The particle sizes of Ni_2P in the NiP/SiO_2-RLP443 and NiP/SiO_2-RLP493 were estimated to be about 6.1 and 8.2 nm, respectively, in agreement with XRD results (see Table 2). In addition, a comparison of TEM images in Fig. 2 (for NiP/SiO_2-DLP493) and Fig. 9 (for NiP/SiO_2-RLP493) clearly demonstrated that the phosphidation after the pre-reduction had the obvious advantages for the production of smaller and more homogeneously dispersed nano Ni_2P particles.

According to the diffraction peaks at 40.7° (Ni_2P (1 1 1)) in the XRD patterns in Fig. 7(a) and Scherrer equation, the average particle sizes of Ni_2P in the series of NiP/SiO_2-RLP catalysts were estimated and given in Table 2. The average size of Ni_2P particles in the NiP/SiO_2-RLP443 was estimated to be 6.2 nm by the Scherrer method, consistent with that determined by TEM. With the increase of phosphidation temperature from 443 to 543 K, the average size of Ni_2P particles in the NiP/SiO_2-RLP-543 as estimated by the Scherrer method increased to 8.4 nm. In contrast, the NiP/SiO_2-DLP543 phosphorized directly at 543 K had the average Ni_2P particle size of 9.2 nm (see Table 1). Thus, the phosphidation after the pre-reduction favored the dispersion of Ni_2P.

Table 2 summarizes the information about the surface areas, pore parameters, crystalline phases, average particle sizes and CO uptakes for the series of NiP/SiO_2-RLP catalysts. With the increase of phosphidation temperature from 393 to 643 K, the surface area (from 220 to 105 m^2/g) and pore volume (from 0.63 to 0.29 cm^3/g) were decreased. As compared with the directly phosphorized samples (NiP/SiO_2-DLP series), both the surface area and pore size were quite different. While the NiP/SiO_2-RLP samples had the surface areas of 220–105 m^2/g and pore sizes of 6.3–9.0 nm, the NiP/SiO_2-DLP samples possessed the surface areas of 172–68 m^2/g and pore sizes of 7.6–17.6 nm. Thus, the NiP/SiO_2-RLP samples phosphorized after the pre-reduction had the higher surface areas but smaller pore sizes than the NiP/SiO_2-DLP samples phosphorized without the pre-reduction, indicating the different changes of the samples under the different phosphidation procedures.

Table 2 also lists the P/Ni atomic ratios for the NiP/SiO_2-RLP samples. The P/Ni ratio was 0.3 for the NiP/SiO_2-RLP393, indicating that the phosphidation of metallic nickel in this sample did occur, but not completely. The P/Ni ratio was increased with the increase of phosphidation temperature. The NiP/SiO_2-RLP443 and NiP/SiO_2-RLP493 had the P/Ni ratios of 0.52 and 0.54, respectively, close to the P/Ni ratio for Ni_2P. The NiP/SiO_2-RLP543 and NiP/SiO_2-RLP643 had the P/Ni ratios of 0.63 and 0.69, respectively, significantly higher than the P/Ni ratio for Ni_2P, in consistence with the XRD result in Fig. 7(a) that showed the presence of quite a few NiP_2 in the sample NiP/SiO_2-RLP643. Although no NiP_2 was detected in the sample NiP/SiO_2-RLP543 (see Fig. 7(a)), the presence of some NiP_2 on the surface of Ni_2P in this sample was highly possible.

The microcalorimetric adsorption of CO was performed on the NiP/SiO_2-RLP catalysts and the results were shown in Fig. 10. The initial heats (92–97 kJ/mol) for the adsorption of CO on the NiP/SiO_2-RLP catalysts phosphorized at the temperatures from 393 to 543 K were similar and significantly lower than that (120 kJ/mol) on the clean surface of nickel powder [43], indicating that the phosphidation of nickel (at least on the surface) in these samples did occur, even though no nickel phosphide species were detected in the NiP/SiO_2-RLP393. It should be noted that the initial heats for the adsorption of CO on the NiP/SiO_2-RLP catalysts (92–97 kJ/mol) were significantly higher than those on the NiP/SiO_2-DLP catalysts (~84 kJ/mol), indicating the different chemical properties of Ni_2P surfaces in the two series of catalysts phosphorized differently. The NiP/SiO_2-RLP643 exhibited the lower initial heat (87 kJ/mol) for the adsorption of CO, probably owing to the presence of NiP_2 on the surface of this sample caused by the high phosphidation temperature (643 K). It should be reasonable that the heat of CO adsorption would be lower on the nickel surfaces with more P atoms.

In addition, the results in Fig. 10 show that the coverage of CO decreased from 465 to 101 μmol/g on the NiP/SiO_2-RLP catalysts when the phosphidation temperature was increased from 393 to 643 K. The coverage of CO must be related to the extent of phosphidation and dispersion of Ni_2P formed. When the phosphidation temperature was low (393 K), the phosphidation process

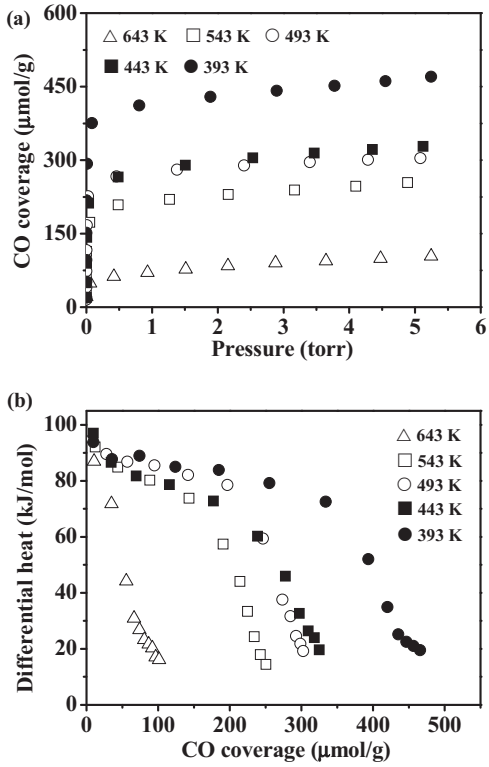

Fig. 10. Isotherms (a) and differential heats (b) measured for the adsorption of CO at 308 K on the Ni_2P/SiO_2 catalysts obtained by the phosphidation of the pre-reduced 60%Ni/SiO_2 (in H_2 at 673 K for 2 h) using PPh_3 in the liquid phase at different temperatures indicated. Before the adsorptions, the samples were re-reduced at 673 K in H_2 for 2 h, followed by the evacuation at 673 K for 1 h.

was incomplete and the particles of Ni and Ni_2P in the NiP/SiO_2-RLP393 must be small, resulting in the high coverage of CO on this sample (465 μmol/g). With the increase of phosphidation temperature, both the extent of phosphidation and particle sizes of formed Ni_2P increased, which had the opposite effects on the CO coverage. When the phosphidation was performed at 443 and 493 K, the resulted catalysts NiP/SiO_2-RLP443 and NiP/SiO_2-RLP493 must have been completely phosphorized and only Ni_2P was formed since they had the P/Ni ratios of 0.52 and 0.54, respectively (see Table 2). In addition, these catalysts contained highly dispersed Ni_2P particles with small diameters (around 6.1 and 7.8 nm, respectively) and thus exhibited the high coverages for the adsorption of CO (324 and 302 μmol/g, respectively). When the phosphidation was carried out at 543 K, the average size of Ni_2P particles formed in the NiP/SiO_2-RLP543 increased to 8.4 nm. This sample possessed the P/Ni ratio of 0.63 (the sign of possible existence of some NiP_2 on the surface), and thus the CO coverage on it was significantly decreased to 250 μmol/g. When the phosphidation was carried out at 643 K, large particles of NiP_2 were formed with Ni_2P in the NiP/SiO_2-RLP643, and thus the sample exhibited the low CO coverage of only 101 μmol/g.

Fig. 11 shows the activities of the NiP/SiO_2-RLP catalysts for the HDS of DBT. The conversion of DBT increased with the increase of reaction temperature until 613 K, at which the conversion of DBT reached 100% on all the NiP/SiO_2-RLP catalysts concerned. Thus, the HDS activities of these catalysts must be compared at the lower reaction temperatures. At 513 K, the conversion of DBT was found to be 70.5, 81.7, 62.2 and 44.1% over the NiP/SiO_2-RLP393, NiP/SiO_2-RLP443, NiP/SiO_2-RLP493 and NiP/SiO_2-RLP543, respectively. Although the NiP/SiO_2-RLP393 exhibited the high CO coverage, the un-phosphorized metallic Ni in this sample might be sulfided into Ni_9S_8 (see Fig. 8) during the hydrotreating

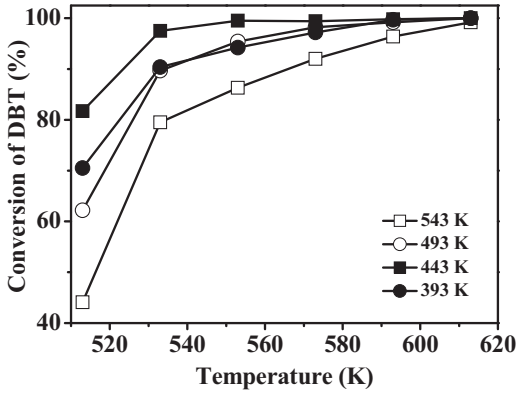

Fig. 11. Conversions of DBT (HDS) on the Ni_2P/SiO_2 catalysts obtained by the phosphidation of pre-reduced 60%Ni/SiO_2 (in H_2 at 673 K for 2 h) using PPh_3 in the liquid phase at different temperatures indicated. Reaction conditions: P = 3.1 MPa, LHSV = 2 h^{-1} and H_2/oil = 1500 (v/v).

reactions, leading to the decreased number of active sites of Ni_2P and thus the lowered HDS activity. Ni_2P was the main phase in the other three catalysts even after the hydrotreating reactions. The conversion of DBT at 513 K on these catalysts decreased with the increase of phosphidation temperature from 443 to 543 K, in consistence with their CO uptakes (i.e., the numbers of active sites of Ni_2P). Among these catalysts, the NiP/SiO_2-RLP443 possessed the most active sites of Ni_2P (324 μmol/g), and thus exhibited the highest activity for the HDS of DBT (81.7%). Among the directly phosphorized catalysts (NiP/SiO_2-DLP series), the NiP/SiO_2-DLP593 exhibited the most active sites of Ni_2P (124 μmol/g) and the highest activity for the HDS of DBT. However, the conversion of DBT at 513 K on the NiP/SiO_2-DLP593 was only 30%. Thus, the Ni_2P/SiO_2 catalysts phosphorized after the pre-reduction were much more active than those phosphorized directly (without the pre-reduction) for the HDS reaction of DBT.

The HDS of DBT usually undergoes through two pathways. One is the direct desulfurization pathway (DDS) with the formation of biphenyl (BP) as the desulfurization product. Another is the indirect desulfurization pathway, i.e., the one for the desulfurization after an aromatic ring in DBT is hydrogenated (HYD), with the formation of cyclohexylbenzene (CHB) as the desulfurization product. The HDS of DBT on the NiP/SiO_2-RLP443 was found to undergo through the two routes, with 56% DDS and 44% HYD pathways, respectively, at 513 K. With the increase of reaction temperature, the HYD route became more important. At 613 K, the HYD and DDS pathways were about 75% and 25%, respectively, on the NiP/SiO_2-RLP443.

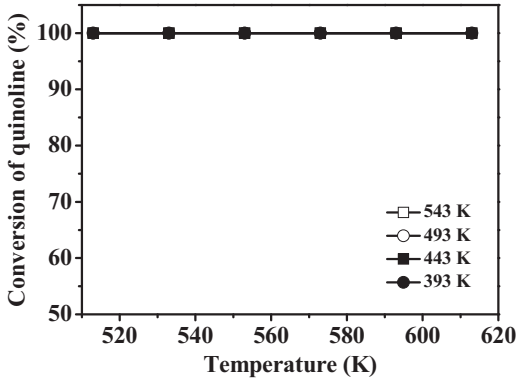

Fig. 12. Conversions of quinoline (HDN) on the Ni_2P/SiO_2 catalysts obtained by the phosphidation of pre-reduced 60%Ni/SiO_2 (in H_2 at 673 K for 2 h) using PPh_3 in the liquid phase at different temperatures indicated. Reaction conditions: P = 3.1 MPa, LHSV = 2 h^{-1} and H_2/oil = 1500 (v/v).

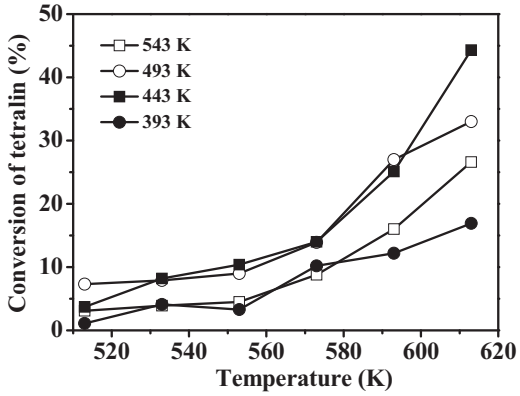

Fig. 13. Conversions of tetralin (hydrogenation) on the Ni_2P/SiO_2 catalysts obtained by the phosphidation of pre-reduced 60%Ni/SiO_2 (in H_2 at 673 K for 2 h) using PPh_3 in the liquid phase at different temperatures indicated. Reaction conditions: P = 3.1 MPa, LHSV = 2 h^{-1} and H_2/oil = 1500 (v/v).

Fig. 12 presents the activities of the NiP/SiO_2-RLP catalysts for the HDN of quinoline. At 513 K, the conversion of quinoline reached 100% on all the NiP/SiO_2-RLP catalysts studied. However, the conversion of quinoline at 513 K on the NiP/SiO_2-DLP593 (the most active one among the series of NiP/SiO_2-DLP catalysts phosphorized directly) was only 56.4%. Thus, the Ni_2P/SiO_2 catalysts phosphorized after the pre-reduction were much more active than those

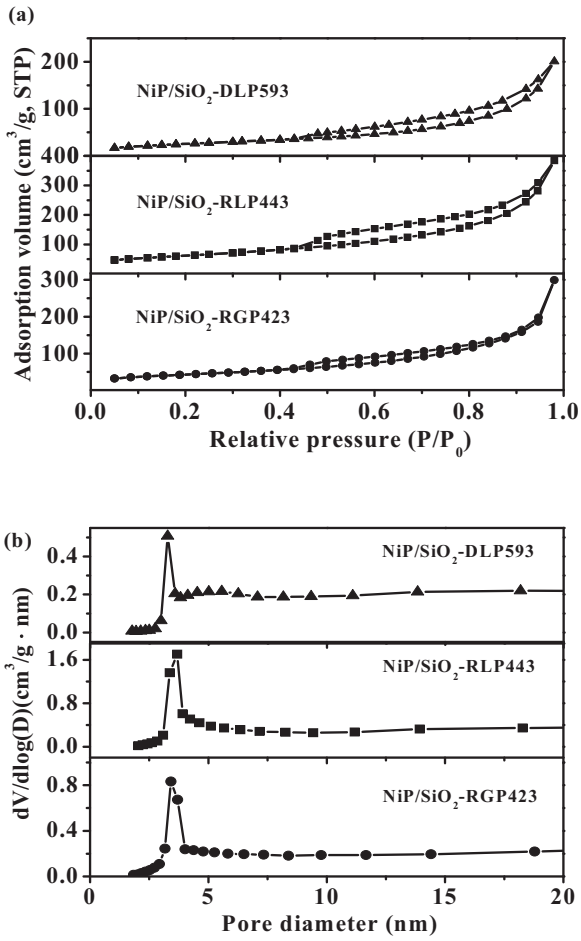

Fig. 14. N_2 adsorption–desorption isotherms (a) and pore size distributions (b) derived from desorption branches of isotherms for the NiP/SiO_2-DLP593, NiP/SiO_2-RLP443 and NiP/SiO_2-RGP423. The reduced samples were passivated in the flow of N_2 containing about 0.5% O_2 at room temperature for 12 h before the measurements.

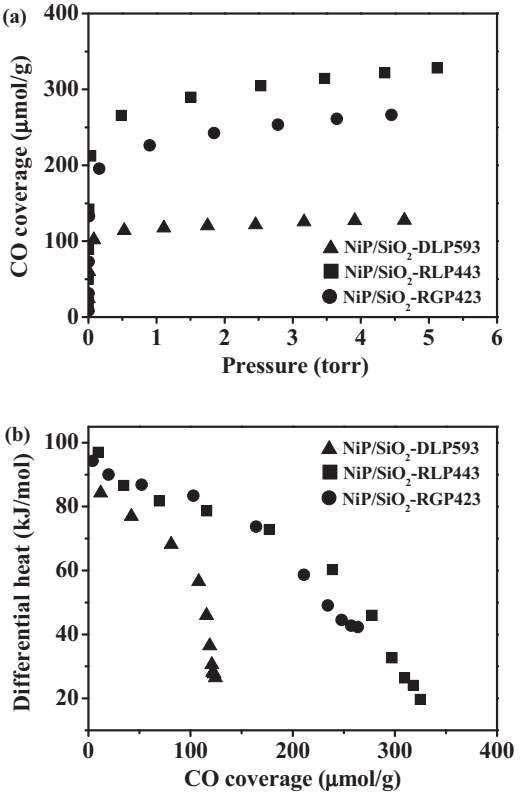

Fig. 15. Isotherms (a) and differential heats (b) measured for the adsorption of CO at 308 K on the catalysts NiP/SiO_2-DLP593, NiP/SiO_2-RLP443 and NiP/SiO_2-RGP423. Before the adsorptions, the samples were re-reduced at 673 K in H_2 for 2 h, followed by the evacuation at 673 K for 1 h.

phosphorized directly (without the pre-reduction) for the HDN reaction of quinoline.

Propylbenzene (PB) and propylcyclohexane (PCH) were the products of HDN of quinoline. At 513 K, the selectivity to PB and PCH were found to be about 21% and 79%, respectively, over the NiP/SiO2-RLP443. The selectivity to PCH increased with reaction temperature. At 613 K, it reached 99% on the NiP/SiO_2-RLP443, i.e., almost all the aromatic rings in quinoline without N atoms were hydrogenated at the relatively high reaction temperature.

Fig. 13 shows the activities of the NiP/SiO_2-RLP catalysts for the hydrogenation of tetralin. At the relatively low temperatures, the conversions of tetralin were low on the NiP/SiO_2-RLP catalysts. The conversion of tetralin was increased with the increase of reaction temperature. At 613 K, the difference in the activity of hydrogenation of tetralin was apparent over the different NiP/SiO_2-RLP catalysts. Since the NiP/SiO_2-RLP393 was only partially phosphorized, metallic nickel in this sample might be sulfided into Ni_9S_8 by DBT during the hydrotreating reactions, and thus this catalyst exhibited the low activity for the hydrogenation of tetralin. The other three catalysts (NiP/SiO_2-RLP443, NiP/SiO_2-RLP493 and NiP/SiO_2-RLP543) contained only the Ni_2P phase and the conversion of tetralin on these catalysts decreased from 44.3 to 26.6% when they were phosphorized at the increased temperatures from 443 to 543 K, in consistence with their densities of surface active sites of Ni_2P (from 324 to 250 μmol/g). Among the directly phosphorized catalysts (NiP/SiO_2-DLP series), the NiP/SiO_2-DLP593 possessed the most active sites of Ni_2P (124 μmol/g) and exhibited the highest activity for the hydrogenation of tetralin. However, the conversion of tetralin at 613 K on the NiP/SiO_2-DLP593 was only 18%. Thus, the Ni_2P/SiO_2 catalysts phosphorized after the pre-reduction were much more active than the directly

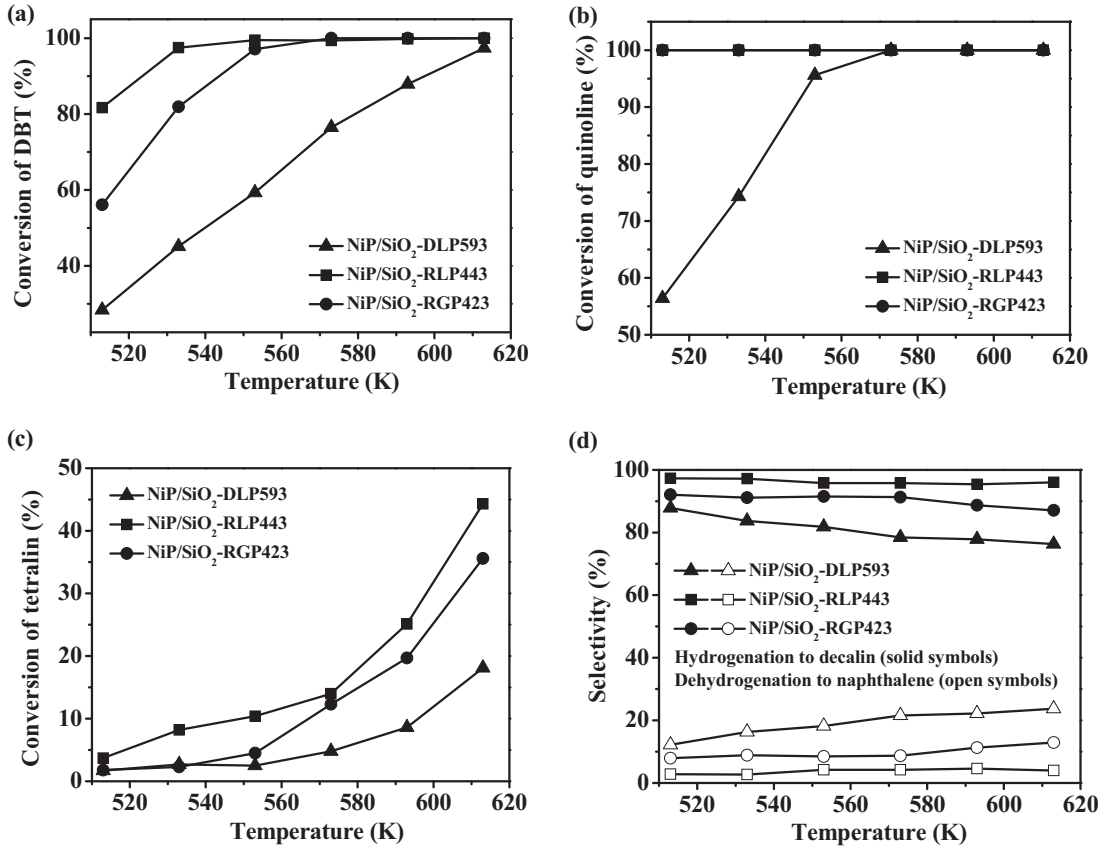

Fig. 16. Conversions of DBT (HDS) (a), quinoline (HDN) (b) and tetralin (hydrogenation and dehydrogenation) (c) on the catalysts NiP/SiO_2-DLP593, NiP/SiO_2-RLP443 and NiP/SiO_2-RGP423. The selectivity to the hydrogenated and dehydrogenated products for the conversion of tetralin is shown in (d). Reaction conditions: P = 3.1 MPa, LHSV = 2 h^{-1} and H_2/oil = 1500 (v/v).

phosphorized ones (without the pre-reduction) for the hydrogenation of tetralin.

3.3. Comparison of different ways of phosphidation

In this section, three Ni_2P/SiO_2 catalysts obtained by the different ways of phosphidation are compared. The precursor was the same (60%Ni/SiO_2) [35]. The first was the Ni_2P/SiO_2 catalyst phosphorized directly at 593 K by PPh_3 in liquid phase without the pre-reduction (NiP/SiO_2-DLP593), which was the most active in this DLP series of catalysts (see Section 3.1 above). The second was the Ni_2P/SiO_2 catalyst phosphorized at 443 K by PPh_3 in liquid phase after the pre-reduction (NiP/SiO_2-RLP443), which was the most active in the RLP series of catalysts (see Section 3.2 above). The third was the Ni_2P/SiO_2 catalyst phosphorized at 423 K by PH_3 in gas phase after the reduction, which was highly active for the HDS and HDN reactions [35] and can be denoted as NiP/SiO_2-RGP423 here.

The three Ni_2P/SiO_2 catalysts were first compared with their textural properties. Fig. 14 shows the N_2 adsorption–desorption isotherms and pore size distribution for the catalysts NiP/SiO_2-DLP593, NiP/SiO_2-RLP443 and NiP/SiO_2-RGP423. Table 3 summarizes their compositions, BET surface areas and pore parameters. These catalysts exhibited the type IV adsorption isotherms with obvious hysteresis loops at relative pressures between 0.43 and 0.95, characteristics of mesopores. The pore sizes were widely distributed with a relatively narrow peak centered at 3.3, 3.6 and 3.4 nm for the NiP/SiO_2-DLP593, NiP/SiO_2-RLP443 and NiP/SiO_2-RGP423, respectively. The data in Table 3 show that the average pore sizes of these catalysts (8.9, 7.7 and 9.9 nm) were much larger than the pore peaks and the differences in pore sizes were not significant. However, the NiP/SiO_2-RLP443 exhibited the significantly larger surface area (220 m^2/g) and pore volume (0.6 cm^3/g) than those of the other two counterparts. This might be an important advantage of liquid phase phosphidation as compared to the gas phase phosphidation for the preparation of Ni_2P/SiO_2 catalysts after the pre-reduction.

Fig. 15 shows the isotherms and differential heats for the adsorption of CO at 308 K on the catalysts NiP/SiO_2-DLP593, NiP/SiO_2-RLP443 and NiP/SiO_2-RGP423. The coverage and initial heat (124 μmol/g and 84 kJ/mol) were relatively low for the adsorption of CO on the NiP/SiO_2-DLP593, while those (263 μmol/g and 94 kJ/mol) were much higher on NiP/SiO_2-RGP423 than on

Table 3
Comparison of Ni_2P/SiO_2 catalysts phosphorized in liquid and gas phases in terms of some of their textural and chemical properties.

Ni_2P/SiO_2 catalyst	NiP/SiO_2-DLP593	NiP/SiO_2-RLP443	NiP/SiO_2-RGP423
S_{BET} (m^2/g)	96	220	152
Pore volume (cm^3/g)	0.31	0.6	0.47
Pore size (nm)	8.9	7.7	9.9
CO uptake (μmol/g)	124	324	263
Ni (wt%)	50.8	47.2	48.2
P (wt%)	10.4	13.1	15.8
P/Ni (atomic ratio)	0.39	0.52	0.62

Note: Data for the NiP/SiO_2-RGP423 were collected from [35].

NiP/SiO_2-DLP593. The NiP/SiO_2-RLP443 exhibited the highest coverage (324 μmol/g) and initial heat (97 kJ/mol) among the three catalysts in comparison for the adsorption of CO. The high coverage and initial heat for the adsorption of CO may explain the high activity of the NiP/SiO_2-RLP443 catalyst for the reactions of HDS, HDN and hydrogenation of tetralin. In fact, the surface density of active sites of Ni_2P (324 μmol/g) as measured by the adsorption of CO was the highest on the NiP/SiO_2-RLP443. No higher value was found in literature so far [35]. This might be another important advantage of liquid phase phosphidation as compared to the gas phase phosphidation for the preparation of Ni_2P/SiO_2 catalysts after the pre-reduction.

Table 3 also gives the data about P/Ni atomic ratios determined by XRF for the three catalysts in comparison. These P/Ni ratios cannot be used alone to judge the extent of phosphidation of the catalysts, since some Ni and P might exist in oxidized states in the catalysts. Thus, other techniques must be used to determine the phases in the catalysts. For example, Ni_2P was the only phase detected by XRD in the catalysts NiP/SiO_2-DLP593, NiP/SiO_2-RLP443 and NiP/SiO_2-RGP423, although they had different P/Ni ratios. The formation of NiP_2 on the surface of Ni_2P was possible in the catalysts with P/Ni ratios significantly higher than 0.5, but was difficult to confirm with the current data. However, the P/Ni ratio significantly lower than 0.5 (for example, 0.39 for the NiP/SiO_2-DLP593) clearly indicated that significant amount of nickel in the NiP/SiO_2-DLP593 was not phosphorized. In addition, it is important to show that the catalyst NiP/SiO_2-RLP443 might have been completely phosphorized (P/Ni = 0.52) for the formation of mainly Ni_2P (XRD) without the sign of presence of NiP_2. The presence of more P than the P/Ni ratio of 0.5 on the surface seemed detrimental to the activity of Ni_2P for the hydrotreating reactions [9].

Fig. 16 compares the catalysts NiP/SiO_2-DLP593, NiP/SiO_2-RLP443 and NiP/SiO_2-RGP423 for the reactions of HDS of DBT, HDN of quinoline and hydrogenation/dehydrogenation of tetralin. Apparently, the NiP/SiO_2-DLP593 was the least active for the reactions since it possessed the lowest density of active sites of Ni_2P (124 μmol/g) among the catalysts in comparison. On the other hand, the NiP/SiO_2-RLP443 was significantly more active than the NiP/SiO_2-RGP423 for the reactions of HDS of DBT and hydrogenation of tetralin (see Fig. 16(a) and (c)), apparently due to that the NiP/SiO_2-RLP443 had the significantly more active sites of Ni_2P (324 μmol/g) than the NiP/SiO_2-RGP423 (263 μmol/g). Both the NiP/SiO_2-RLP443 and NiP/SiO_2-RGP423 exhibited the 100% conversion of quinoline under the reaction conditions employed, indicating that such reaction conditions could not distinguish the difference of activity of the two catalysts for the HDN of quinoline. More importantly, the NiP/SiO_2-RLP443 exhibited the highest selectivity (>95.4%) to decalin, the hydrogenation product of tetralin with little selectivity (<4.6%) to naphthalene, the dehydrogenation product of tetralin. In contrast, the selectivity to the dehydrogenation product might be as high as 12.9% and 23.7% on the NiP/SiO_2-RGP423 and NiP/SiO_2-DLP593, respectively. Since the saturation of multi-rings of aromatic compounds in diesel fuels is highly desirable, the high activity of the NiP/SiO_2-RLP443 catalyst for the hydrogenation of tetralin might be its unique feature that can be used to increase the cetane number of diesel fuels during their hydrotreating reactions.

4. Conclusions

A highly loaded (60%Ni) and dispersed Ni/SiO_2 catalyst (800 μmol/g for the adsorption of H_2) was phosphorized by PPh_3 in liquid phase for the preparation of highly loaded and dispersed Ni_2P/SiO_2 catalysts, and compared with the Ni_2P/SiO_2 catalyst (NiP/SiO_2-RGP423) obtained by the phosphidation of the same Ni/SiO_2 catalyst with PH_3 at 423 K in gas phase [35].

It was found that without the pre-reduction, the Ni/SiO_2 could not be completely phosphorized by PPh_3 in liquid phase even at the temperature as high as 593 K, and the resulted catalyst NiP/SiO_2-DLP593 possessed the low content of Ni_2P, large sizes of Ni_2P particles and thus the relatively low density of active sites of Ni_2P (124 μmol/g) as measured by the adsorption of CO. Such catalysts obtained by the direct phosphidation in liquid phase exhibited the relatively low activity for the HDS of DBT, HDN of quinoline and hydrogenation of tetralin.

On the other hand, when the Ni/SiO_2 was pre-reduced, the highly dispersed nano nickel particles formed during the reduction were easily phosphorized by PPh_3 in liquid phase even at the temperature as low as 443 K for the formation of highly dispersed Ni_2P particles. XRD and XRF results indicated the complete phosphidation in this case, without the excessive deposition of P. The resulted catalyst NiP/SiO_2-RLP443 possessed the high content of Ni_2P, small and homogeneously distributed Ni_2P particles (~6 nm), and thus the high density of active sites of Ni_2P (324 μmol/g) as measured by the adsorption of CO. Such catalysts obtained by the phosphidation of pre-reduced Ni/SiO_2 in liquid phase exhibited the high activity for the HDS of DBT, HDN of quinoline and hydrogenation of tetralin.

Industrially, the hydrotreating catalysts Co—Mo—S and Ni—Mo—S were sulfided either by H_2S in gas phase or by CS_2 in liquid phase. Previously, we showed that the highly active hydrotreating catalyst Ni_2P/SiO_2 (NiP/SiO_2-RGP423) could be prepared by the gas phase phosphidation with PH_3 [35]. The current work provided another option of liquid phase phosphidation with PPh_3 whenever it is needed. In particular, the NiP/SiO_2-RLP443 catalyst phosphorized in liquid phase possessed significantly more active sites of Ni_2P (324 μmol/g), and thus significantly more active for the reactions of HDS of DBT and hydrogenation of tetralin to decalin, than the NiP/SiO_2-RGP423 catalyst phosphorized in gas phase (263 μmol/g).

Acknowledgments

Financial supports from NSFC (21273105), MSTC (2013AA031703) and the fundamental research funds for central universities (1084020501) are acknowledged.

References

[1] W. Fu, L. Zhang, T. Tang, Q. Ke, S. Wang, J. Hu, G. Fang, J. Li, F.-S. Xiao, J. Am. Chem. Soc. 133 (2011) 15346–15349.
[2] S.T. Oyama, J. Catal. 216 (2003) 343–352.
[3] S.T. Oyama, H.Y. Zhao, H.J. Freund, K. Asakura, R. Wlodarczyk, M. Sierka, J. Catal. 285 (2012) 1–5.
[4] V. Zuzaniuk, R. Prins, J. Catal. 219 (2003) 85–96.
[5] S.J. Sawhill, D.C. Phillips, M.E. Bussell, J. Catal. 215 (2003) 208–219.
[6] C.M. Sweeney, K.L. Stamm, S.L. Brock, J. Alloys Compd. 448 (2008) 122–127.
[7] V. Teixeira da Silva, L.A. Sousa, R.M. Amorim, L. Andrini, S.J.A. Figueroa, F.G. Requejo, F.C. Vicentini, J. Catal. 279 (2011) 88–102.
[8] S.F. Yang, C.H. Liang, R. Prins, J. Catal. 237 (2006) 118–130.
[9] S.J. Sawhill, K.A. Layman, D.R. Van Wyk, M.H. Engelhard, C. Wang, M.E. Bussell, J. Catal. 231 (2005) 300–313.
[10] G. Shi, J. Shen, Catal. Commun. 10 (2009) 1693–1696.
[11] G. Shi, J. Shen, J. Mater. Chem. 19 (2009) 2295–2297.
[12] Q. Guan, W. Li, M. Zhang, K. Tao, J. Catal. 263 (2009) 1–3.
[13] B.M. Barry, E.G. Gillan, Chem. Mater. 20 (2008) 2618–2620.
[14] H. Hou, Q. Peng, S. Zhang, Q. Guo, Y. Xie, Eur. J. Inorg. Chem. 2005 (2005) 2625–2630.
[15] Y. Xie, H.L. Su, X.F. Qian, X.M. Liu, Y.T. Qian, J. Solid State Chem. 149 (2000) 88–91.
[16] C.S. Blackman, C.J. Carmalt, S.A. O'Neill, I.P. Parkin, L. Apostolico, K.C. Molloy, Appl. Surf. Sci. 211 (2003) 2–5.
[17] S.C. Perera, G. Tsoi, L.E. Wenger, S.L. Brock, J. Am. Chem. Soc. 125 (2003) 13960–13961.
[18] S.C. Perera, P.S. Fodor, G.M. Tsoi, L.E. Wenger, S.L. Brock, Chem. Mater. 15 (2003) 4034–4038.
[19] A.E. Henkes, Y. Vasquez, R.E. Schaak, J. Am. Chem. Soc. 129 (2007) 1896–1897.
[20] A.E. Henkes, R.E. Schaak, Chem. Mater. 19 (2007) 4234–4242.

[21] C. Qian, F. Kim, L. Ma, F. Tsui, P. Yang, J. Liu, J. Am. Chem. Soc. 126 (2004) 1195–1198.
[22] J. Park, B. Koo, Y. Hwang, C. Bae, K. An, J.-G. Park, H.M. Park, T. Hyeon, Angew. Chem. Int. Ed. 43 (2004) 2282–2285.
[23] H. Zhang, D.-H. Ha, R. Hovden, L.F. Kourkoutis, R.D. Robinson, Nano Lett. 11 (2010) 188–197.
[24] X. Zheng, S. Yuan, Z. Tian, S. Yin, J. He, K. Liu, L. Liu, Mater. Lett. 63 (2009) 2283–2285.
[25] X. Zheng, S. Yuan, Z. Tian, S. Yin, J. He, K. Liu, L. Liu, Chem. Mater. 21 (2009) 4839–4845.
[26] R. Prins, M.E. Bussell, Catal. Lett. 142 (2012) 1413–1436.
[27] K. Senevirathne, A.W. Burns, M.E. Bussell, S.L. Brock, Adv. Funct. Mater. 17 (2007) 3933–3939.
[28] K.-S. Cho, H.-R. Seo, Y.-K. Lee, Catal. Commun. 12 (2011) 470–474.
[29] G.H. Layan Savithra, E. Muthuswamy, R.H. Bowker, B.A. Carrillo, M.E. Bussell, S.L. Brock, Chem. Mater. 25 (2013) 825–833.
[30] G. Shi, D. Fang, J. Shen, Microporous Mesoporous Mater. 120 (2009) 339–345.
[31] G. Shi, H. Zhao, L. Song, J. Shen, Energy Fuels 22 (2008) 2450–2454.
[32] Y. Li, D. Pan, C. Yu, Y. Fan, X. Bao, J. Catal. 286 (2012) 124–136.
[33] A.E. Coumans, D.G. Poduval, J.A.R. van Veen, E.J.M. Hensen, Appl. Catal., A: Gen. 411 (2012) 51–59.
[34] D. Ferdous, N.N. Bakhshi, A.K. Dalai, J. Adjaye, Appl. Catal., B: Environ. 72 (2007) 118–128.
[35] Y. Zhao, M. Xue, M. Cao, J. Shen, Appl. Catal., B: Environ. 104 (2011) 229–233.
[36] M. Xue, S. Hu, H. Chen, Y. Fu, J. Shen, Catal. Commun. 12 (2011) 332–336.
[37] S.L. Brock, K. Senevirathne, J. Solid State Chem. 181 (2008) 1552–1559.
[38] E. Muthuswamy, S.L. Brock, J. Am. Chem. Soc. 132 (2010) 15849–15851.
[39] S.T. Oyama, Y.-K. Lee, J. Catal. 258 (2008) 393–400.
[40] Y. Zhao, Y. Zhao, H. Feng, J. Shen, J. Mater. Chem. 21 (2011) 8137–8145.
[41] M. Santikunaporn, J.E. Herrera, S. Jongpatiwut, D.E. Resasco, W.E. Alvarez, E.L. Sughrue, J. Catal. 228 (2004) 100–113.
[42] A.E. Nelson, M. Sun, A.S.M. Junaid, J. Catal. 241 (2006) 180–188.
[43] J. Shen, B.E. Spiewak, J.A. Dumesic, Langmuir 13 (1997) 2735–2739.